



# Pathological and phylogenetic characterization of a rare fowl adenovirus (FAdV-8b) associated with inclusion body hepatitis in naturally infected *Meleagris gallopavo*

Shady Shalaby<sup>1</sup> · Walaa Awadin<sup>1</sup> · Reham Karam<sup>2</sup> · Sanaa Salem<sup>3</sup> · Ahmed El-Shaieb<sup>1,4</sup>

Received: 7 February 2024 / Accepted: 11 April 2024 / Published online: 12 June 2024  
© The Author(s), under exclusive licence to Springer-Verlag GmbH Austria, part of Springer Nature 2024

## Abstract

Adenoviruses are a diverse group of viruses that can cause a variety of diseases in poultry, including respiratory and gastrointestinal infections. In turkeys (*Meleagris gallopavo*), adenoviruses commonly cause hemorrhagic enteritis and, rarely, inclusion body hepatitis. In this study, we investigated fowl adenoviruses (FAdVs) circulating in turkeys in Egypt. Following clinical examination of 500 birds, a portion of the hexon gene was amplified from four out of 50 samples from diseased birds (8%), and one amplicon that produced a strong band was selected for sequencing. Molecular and phylogenetic analysis revealed that the virus in that sample belonged to serotype FAdV-8b. Histopathological and immunohistochemical examinations of prepared tissue sections were performed to confirm the pathological findings. Diseased birds exhibited ruffled feathers, low body weight, a crouching posture, and diarrhea. Gross examination revealed petechial hemorrhage on the spleen, swollen pale liver, and congested intestine. Microscopic examination revealed the presence of eosinophilic and basophilic intranuclear inclusion bodies, nuclear pyknosis, and apoptotic bodies in the liver, congestion, hemorrhage, and fibrosis in the lungs, and desquamation of enterocytes. The presence of viral antigens in the liver, lungs, and intestine was confirmed by immunohistochemistry. To our knowledge, this is the first report of the characterization of an outbreak of inclusion body hepatitis in turkeys (hybrid converter breeds) due to FAdV-8b in Egypt. This finding raises an epidemiological alarm, necessitating further studies, including full-genome sequencing, to trace the virus's origin and genetic diversity.

## Introduction

Turkeys are an ideal source of meat in many countries due to their high level of production and their nutritional value. These advantages are challenged by viral infections, which cause great losses [1]. One of the viruses causing significant disease in turkeys is fowl adenovirus (FAdV), which is a dsDNA virus belonging to the genus *Aviadenovirus* of the family *Adenoviridae*. The FAdVs are subdivided into five species (*Aviadenovirus ventriculi*, *Aviadenovirus quintum*, *Aviadenovirus hydropericardii*, *Aviadenovirus gallinae*, and *Aviadenovirus hepatitisidis*) and 12 serotypes [2–5]. The 12 serotypes (FAdV-1 to 8a and 8b to 11) were identified by cross-neutralization tests using antibodies to the hexon protein. FAdV-2, FAdV-8a, FAdV-8b, and FAdV-11 can cause inclusion body hepatitis (IBH), while FAdV-4 causes hepatitis hydropericardium syndrome (HHS) and FAdV-1 causes adenoviral gizzard erosions [6, 7].

---

Communicated by Eric J Kremer

✉ Shady Shalaby  
shadyshalaby25@mans.edu.eg

✉ Walaa Awadin  
awadin@mans.edu.eg

<sup>1</sup> Department of Pathology, Faculty of Veterinary Medicine, Mansoura University, Mansoura 35516, Egypt

<sup>2</sup> Department of Virology, Faculty of Veterinary Medicine, Mansoura University, Mansoura 35516, Egypt

<sup>3</sup> Department of Pathology, Animal Health Research Institute (AHRI), Zagazig Branch, Agriculture Research Centre (ARC), Zagazig 44516, Egypt

<sup>4</sup> Department of Pathology, Faculty of Veterinary Medicine, Egyptian Chinese University, Cairo, Egypt

IBH is characterized by a sudden increase in mortality, which can reach up to 30% within a flock, and low morbidity. Diseased young broiler chickens exhibit ruffled feathers, growth retardation, and a crouching posture. The disease is more intense in young birds during the first few days of life. However, the infection might be subclinical and only noticed at the slaughterhouse [2, 3].

The main lesions of IBH observed in turkeys are friable, pale, swollen livers with petechial hemorrhage and small white foci on the liver, swollen kidneys, and atrophied bursa and thymus [2, 3, 8]. Microscopically, intranuclear inclusion bodies (INIBs) are found in the liver, pancreas, intestine, gizzard, and kidneys. The INIBs are mainly basophilic, round or irregular, large bodies with a clear pale halo in the early stage, while in the later stage, they are eosinophilic without virus particles [9]. Hepatitis with multifocal areas of coagulative necrosis, glomerulonephritis, pancreatitis, cholangitis, and cholecystitis with mononuclear cell infiltration has been reported [2, 3, 8, 10].

In the intestine, mucosal congestion, epithelial necrosis, and hemorrhage in villus tips due to endothelial disruption are observed, while blood vessels appear to be intact, and RBC diapedesis is observed. Mononuclear cell infiltration is evident in the lamina propria. Intestinal lesions are severe in the duodenum and less severe in the distal parts [4, 11].

Amplification of the hexon gene by PCR is considered the most practical method of detection of adenoviruses. Other, older methods, including virus isolation, immunohistochemical staining, *in situ* hybridization, and serotyping by virus neutralization, are still used in many laboratories [2, 4, 8, 10].

This study is a retrospective investigation of adenoviruses circulating among turkeys in the delta region of northern Egypt in 2023. A rare FAdV infection leading to IBH was identified, and the associated virus was characterized phylogenetically, pathologically, and immunohistochemically.

## Materials and methods

### Sampling

To investigate the presence of FAdV on turkey farms on which hybrid converter breeds are raised, about 500 birds in the delta region of northern Egypt were examined in 2023. Of the birds tested, 95% were less than 6 weeks old and had no history of adenovirus vaccination. Clinical examination revealed that 50 of the birds were diseased, and these were euthanized and necropsied, and gross lesions were recorded. Representative tissue samples were taken from lungs, trachea, liver, kidneys spleen, heart, and intestine from all 50

necropsied birds, and particular emphasis was placed on the examination of respiratory and intestinal organs.

Tissue samples were divided into two portions, one of which was preserved at  $-20^{\circ}\text{C}$  and then homogenized in phosphate-buffered saline (PBS) (pH 7.4) to make a 10% suspension, which was then clarified in a benchtop microfuge at 2000 rpm for 10 minutes, and 200  $\mu\text{l}$  of the supernatant from each sample pool was used for extraction of viral DNA. The other portion of the tissue was preserved in 10% buffered formalin for histopathological and immunohistochemistry (IHC) investigation.

### Extraction of nucleic acids

Nucleic acids were extracted using a QIAamp Viral DNA Extraction Kit, (QIAGEN, USA; catalogue no.51304) according to the manufacturer's protocol. Viral DNA was kept at  $-20^{\circ}\text{C}$  until used.

### PCR amplification of a portion of the hexon gene of fowl adenovirus

A 727-bp region of the hexon gene was amplified by PCR to confirm the presence of viral DNA and for sequencing. The forward primer was adeno-F (5'-ACATGGGAGCGA CCTACTTCGACA-3) and the reverse primer was adeno-R (5'- TCGGCGAGCATGTACTGGTAAAC-3) [12]. The oligonucleotide primers were obtained from Metabion (Germany). The PCR reaction mixture consisted of 12.5  $\mu\text{l}$  of 2 $\times$  Emerald Amp GT PCR master mix (Takara, no. RR310A), 1  $\mu\text{l}$  of forward primer (20 pmol), 1  $\mu\text{l}$  of reverse primer (20 pmol), 4.5  $\mu\text{l}$  of PCR-grade water, and 6  $\mu\text{l}$  of template DNA to give a total volume of 25  $\mu\text{l}$ . Field isolates supplied by the reference laboratory of the Animal Health Research Institute, Dokki, Giza, Egypt, were used as positive controls, and nuclease-free water was used as a negative control.

Amplification was carried out in a Chromo4 Thermal Cycler (Bio-Rad, Hercules, CA, USA). The cycling conditions were 5 min at  $94^{\circ}\text{C}$  for primary denaturation, followed by 35 cycles of secondary denaturation at  $94^{\circ}\text{C}$  for 30 s, annealing at  $60^{\circ}\text{C}$  for 40 s, and extension at  $72^{\circ}\text{C}$  for 45 s, and a final extension at  $72^{\circ}\text{C}$  for 10 min. Amplification products were subjected to 1.5% agarose gel electrophoresis, excised from the gel, and kept at  $-20^{\circ}\text{C}$  before purification.

### Agarose gel electrophoresis

As described by Falcone et al. [13], agarose gels were prepared by dissolving 0.45 of agarose powder in 30 ml of TBE buffer by heating on a flame and then cooling to  $55^{\circ}\text{C}$ , and 5  $\mu\text{l}$  of ethidium bromide was added to a final concentration

of 0.5 µg/ml. A GeneRuler 100 bp DNA Ladder (Fermentas, cat. no. SM0243) was used as a size marker.

### Purification of PCR products for sequencing

PCR products were purified using a QIAquick PCR Purification Kit (QIAGEN Inc., Valencia, CA) (catalogue no. 28104) according to the manufacturer's instructions.

### Sequencing and phylogenetic analysis

Purified PCR products were sequenced using an Applied Biosystems 3130 Genetic Analyzer (ABI, 3130, USA). The sequence reactions were carried out according to the manufacturer's instructions, using a BigDye Terminator V3.1 Cycle Sequencing Kit (PerkinElmer/Applied Biosystems, Foster City, CA). Similar sequences in the GenBank database were identified using the Basic Local Alignment Search Tool (BLAST) [14]. The nucleotide sequence from this study has been deposited in the GenBank database under the accession number OR495594.

A multiple alignment of partial hexon amino acid sequences was made by the CLUSTAL W method [17, 18], using the MegAlign module of Lasergene DNASTAR software (Madison, Wisconsin, USA), and phylogenetic analysis was performed in MEGA 11 [15] by the neighbor-joining method with the Tajima-Nei model and 1000 bootstrap replicates [16].

### Histopathological examination

For pathological investigation, formalin-fixed tissue specimens were placed in cassettes, treated with ethanol and xylene, and embedded in melted paraffin. Serial sections of 4–5 µm were cut for hematoxylin and eosin (H&E) staining and IHC using a microtome then placed on clean glass slides. At the time of staining, the slides were dewaxed, rehydrated, stained with H&E, and mounted with quick mount. The stained slides were then examined using a light microscope [19].

### Immunohistochemistry (IHC)

IHC was performed as described by Suvarna et al. [20] to confirm the presence of adenovirus and to determine which tissues were affected. The procedure was implemented over two days. On the first day, paraffin sections of PCR-confirmed cases were dewaxed, rehydrated, and washed three times with PBS before antigen retrieval by autoclaving at 120°C for 20 min and washing three times with PBS. After that, 5% hydrogen peroxide was applied, and the slides were incubated for 30 min at room temperature and then washed

with PBS. Primary polyclonal chicken antibodies specific for adenovirus (kindly provided by the reference laboratory of the Animal Health Research Institute, Dokki, Giza, Egypt) were diluted 1:100 in Ab dilution buffer, applied to the sample, and incubated at 4°C overnight.

On the second day, secondary biotinylated antibodies (kindly provided by the reference laboratory of the Animal Health Research Institute, Dokki, Giza, Egypt) were applied, and the sample was incubated for 1 h. Streptavidin horseradish peroxidase was then applied, and the slides were kept at room temperature for 60 min and then washed. The slides were stained with DAP and then counterstained with hematoxylin [21].

## Results

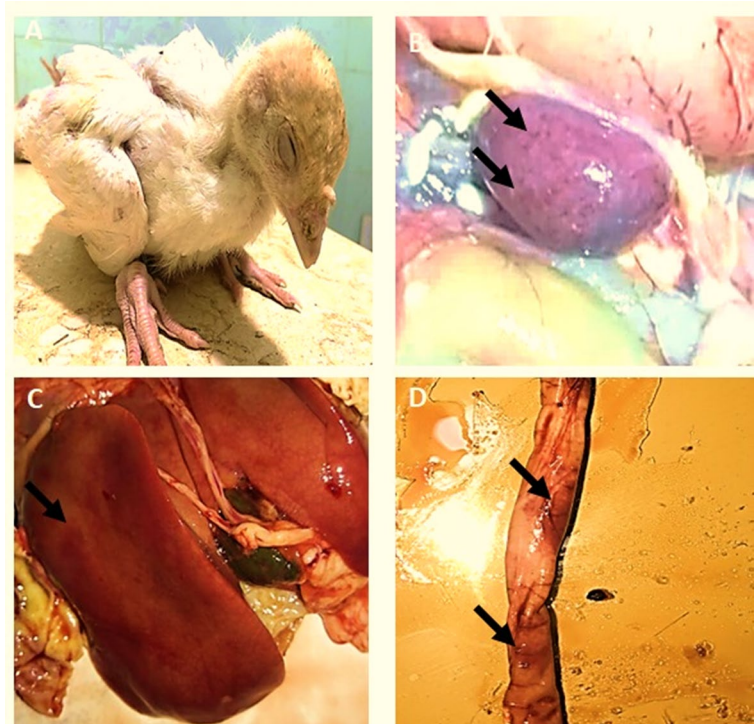
### Clinical signs and gross lesions

Most of the diseased birds in this study exhibited lethargy, ruffled feathers, low body weight, a crouching posture, and diarrhea, but a few showed difficulty breathing, nasal discharge, and rales. A gross postmortem examination revealed splenomegaly with petechial hemorrhage, swollen pale liver, and congested intestine (Fig. 1).

### Molecular characterization and sequence analysis

The hexon gene was successfully amplified from four samples (8%), and one amplicon that produced a strong band in an agarose gel was sequenced in both directions. This partial hexon gene sequence was submitted to the GenBank database under the accession number OR495594. Sequence analysis revealed that this virus belongs to serotype FAdV-8b and is a member of the species *Aviadenovirus hepatitidis*. The sequenced region of the isolate from Egypt (EGYAD OR495594) was 100% identical to the corresponding region from isolates of chickens in Australia in 2022 (MT459118) and 2021 (MT459112, MT459113, and MT459114) and ≥98.7% identical to those found in isolates from chickens in Egypt in 2022 (MW712887 and MW712888), Malaysia in 2016 (KU517714), and Slovenia in 2016 (JF766221) (Fig. 2). The nucleotide sequence alignment revealed high similarity of the EGYAD isolate to the isolates AD15 and AD16 (Fig. 3). The predicted amino acid sequences were identical to those reported recently isolated in chickens in Egypt, but a few amino acids differed from the reference strains (Fig. 4). A phylogenetic tree based on the hexon gene of fowl adenoviruses was constructed by the neighbor-joining method and is shown in Fig. 5.

**Fig. 1** Clinical signs and gross findings in poult infected with fowl adenovirus. **(A)** A weak, emaciated poult in a crouching position. **(B)** Splenomegaly with petechial hemorrhage (black arrows). **(C)** Swollen pale liver (black arrow). **(D)** A congested intestine (black arrows)



		Percent Identity																							
		1	2	3	4	5	6	7	8	9	10	11	12	13	14	15	16	17	18	19	20	21	22	23	
Divergence	1	57.9	58.7	66.2	62.1	60.8	62.6	61.6	60.3	60.5	60.7	60.3	59.2	59.2	60.5	60.5	60.5	60.3	60.5	60.5	58.9	66.2	58.9	1	
	2	57.4	72.3	55.9	64.6	70.7	68.9	70.2	68.0	68.2	67.9	67.7	68.7	68.7	68.2	68.2	68.2	68.0	68.0	68.2	72.6	56.2	94.6	2	
	3	55.2	35.0	55.7	63.1	69.8	68.2	66.7	68.0	68.2	68.2	68.2	68.4	68.4	68.2	68.2	68.2	68.4	68.0	68.2	94.8	56.1	73.4	3	
	4	42.4	60.5	60.0	59.8	59.7	60.7	60.0	59.0	58.9	58.7	58.9	58.4	58.4	58.9	58.9	58.9	58.9	58.7	58.9	58.9	55.7	95.9	56.4	4
	5	49.5	46.4	48.8	52.7	67.7	67.2	68.2	65.1	65.2	64.8	65.1	65.2	65.2	65.2	65.2	65.2	65.1	65.1	65.2	62.8	59.3	64.1	5	
	6	51.9	37.6	38.5	52.5	41.5	84.3	82.3	79.5	79.7	79.8	80.0	80.5	80.5	79.7	79.7	79.8	79.5	79.7	79.8	69.5	59.3	71.1	6	
	7	48.7	40.1	40.9	50.2	41.8	17.5	83.1	87.5	87.7	87.4	88.0	88.2	88.2	87.7	87.7	87.7	87.5	87.5	87.7	68.9	60.3	68.7	7	
	8	50.3	38.5	44.4	52.0	40.5	20.8	18.9	81.6	81.8	80.2	80.5	80.5	80.5	81.8	81.8	81.8	81.6	81.6	81.8	65.9	60.0	70.0	8	
	9	53.0	42.4	41.6	54.0	46.2	24.6	13.4	21.5	99.8	97.9	98.5	96.6	96.6	99.8	99.8	99.8	99.7	99.7	99.8	68.2	59.0	68.0	9	
	10	52.7	42.1	41.3	54.4	45.9	24.4	13.2	21.3	0.2	98.0	98.7	96.7	96.7	100.0	100.0	100.0	99.8	99.8	100.0	68.4	58.9	68.2	10	
	11	52.2	42.5	41.1	54.5	46.7	24.0	13.4	23.4	2.0	1.9	99.0	96.9	96.9	98.0	98.0	98.0	97.9	97.9	98.0	68.4	58.9	67.7	11	
	12	53.0	43.1	41.3	54.4	46.2	23.9	12.8	23.1	1.5	1.3	0.8	97.4	97.4	98.7	98.7	98.7	98.5	98.5	98.7	68.4	59.0	67.7	12	
	13	55.5	41.1	41.0	55.3	45.9	23.2	12.5	23.0	3.6	3.4	3.1	2.7	100.0	96.7	96.7	96.7	96.6	96.6	96.7	68.7	58.7	68.2	13	
	14	55.5	41.1	41.0	55.3	45.9	23.2	12.5	23.0	3.6	3.4	3.1	2.7	0.0	96.7	96.7	96.7	96.6	96.6	96.7	68.7	58.7	68.2	14	
	15	52.7	42.1	41.3	54.4	45.9	24.4	13.2	21.3	0.2	0.0	1.9	1.3	3.4	3.4	100.0	100.0	99.8	99.8	100.0	68.4	58.9	68.2	15	
	16	52.7	42.1	41.3	54.4	45.9	24.4	13.2	21.3	0.2	0.0	1.9	1.3	3.4	3.4	0.0	100.0	99.8	99.8	100.0	68.4	58.9	68.2	16	
	17	52.7	42.1	41.3	54.4	45.9	24.4	13.2	21.3	0.2	0.0	1.9	1.3	3.4	3.4	0.0	0.0	99.8	99.8	100.0	68.4	58.9	68.2	17	
	18	53.1	42.4	41.0	54.4	46.2	24.1	13.4	21.5	0.3	0.2	2.0	1.5	3.6	3.6	0.2	0.2	0.2	99.7	99.8	68.5	58.9	68.0	18	
	19	52.7	42.4	41.6	54.7	46.2	24.6	13.4	21.5	0.3	0.2	2.0	1.5	3.6	3.6	0.2	0.2	0.2	0.3	99.8	68.2	58.7	68.0	19	
	20	52.7	42.1	41.3	54.4	45.9	24.4	13.2	21.3	0.2	0.0	1.9	1.3	3.4	3.4	0.0	0.0	0.0	0.2	0.2	68.4	58.9	68.2	20	
	21	55.3	35.0	5.1	60.7	50.1	39.6	40.2	46.5	41.8	41.5	41.3	41.5	40.9	40.9	41.5	41.5	41.5	41.2	41.8	41.5	56.2	74.1	21	
	22	42.4	59.8	59.2	4.4	53.9	53.3	50.9	52.2	54.2	54.5	54.3	54.2	54.8	54.8	54.5	54.5	54.5	54.5	54.9	54.5	59.5	56.4	22	
	23	55.1	5.7	33.1	59.1	47.3	36.7	40.3	38.8	42.2	41.9	42.7	42.9	41.9	41.9	41.9	41.9	41.9	42.2	42.2	41.9	32.6	59.2	23	
	1	2	3	4	5	6	7	8	9	10	11	12	13	14	15	16	17	18	19	20	21	22	23		

MF198255 FAdV-1 SDJN  
 ON502482 FAdV-2/Hubei/ch/H2054/2019  
 AF508948 FAdV-3 SR49  
 AF339917 FAdV-4 ATCC VR-829  
 AF508952 FAdV-5 340  
 AF508954 FAdV-6 CR119  
 KT862809 FAdV-7 YR36  
 OQ132924 FAdV-8a UDLA 17  
 KU517714 FAdV-8b UPM04217  
 MT459118 FAdV-8b D4  
 MT459111 FAdV-8b B2/2  
 JF766221 FAdV-8b  
 OL456208 FAdV-8b SD2009  
 OK188966 FAdV-8b HeB20  
 MT459114 FAdV-8b B2/5  
 MT459113 FAdV-8b B2/4  
 MT459112 FAdV-8b B2/3  
 MW712888 FAdV-8b AD15  
 MW712887 FAdV-8b AD16  
 OR495594 FAdV-8b-EGYAD ★  
 NC\_000899 FAdV-9  
 ON502597 FAdV-10/Anhui/ch/A2036/2019  
 ON462366 FAdV-11/Hubei/ch/H2218/2019

**Fig. 2** Percent sequence identity in the hexon gene between the EGYAD sample and other sequences obtained from the GenBank database. EGYAD is indicated by a star

**Histopathological and immunohistochemical examination**

Microscopic examination of formalin-fixed samples collected from birds that were adenovirus positive by PCR is presented in Fig. 6A-D, Fig. 7A-C, and Fig. 8A-E. The trachea showed moderate hyperplasia of goblet cells with heterophil infiltration. The lungs showed congestion,

haemorrhage, perivascular fibrosis, fibrosis in the alveolar wall, and multiple foci of leukocytic cell aggregation. The liver showed a fatty change in hepatocytes, eosinophilic and basophilic INIBs, nuclear pyknosis, and apoptotic bodies. The kidneys showed marked congestion, interstitial edema, fibrosis, and follicular aggregation of lymphocytes. The heart showed interstitial edema. The spleen showed a depletion of lymphocytes from the white pulp. The small

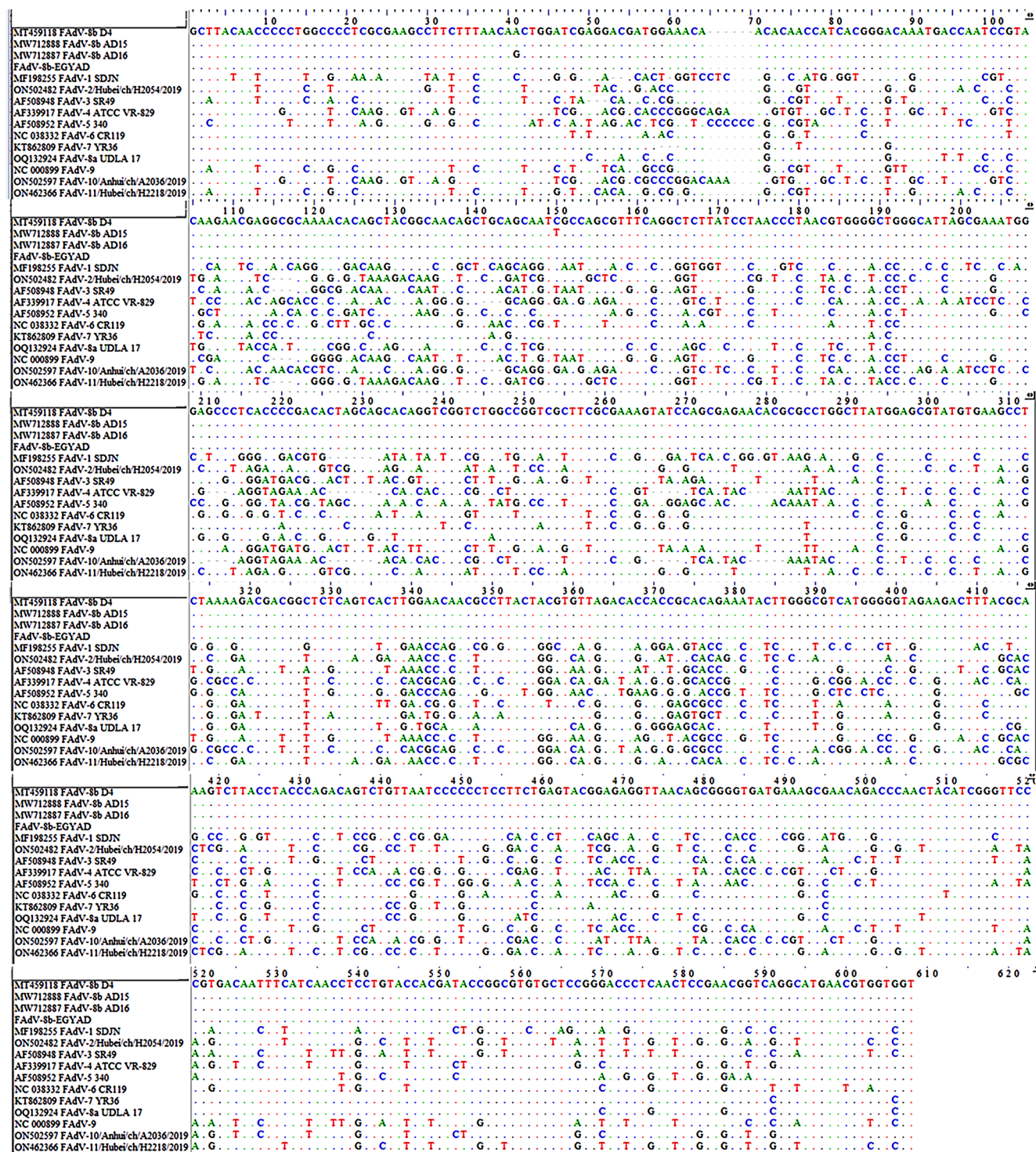


Fig. 3 Multiple alignment of FAdV sequences

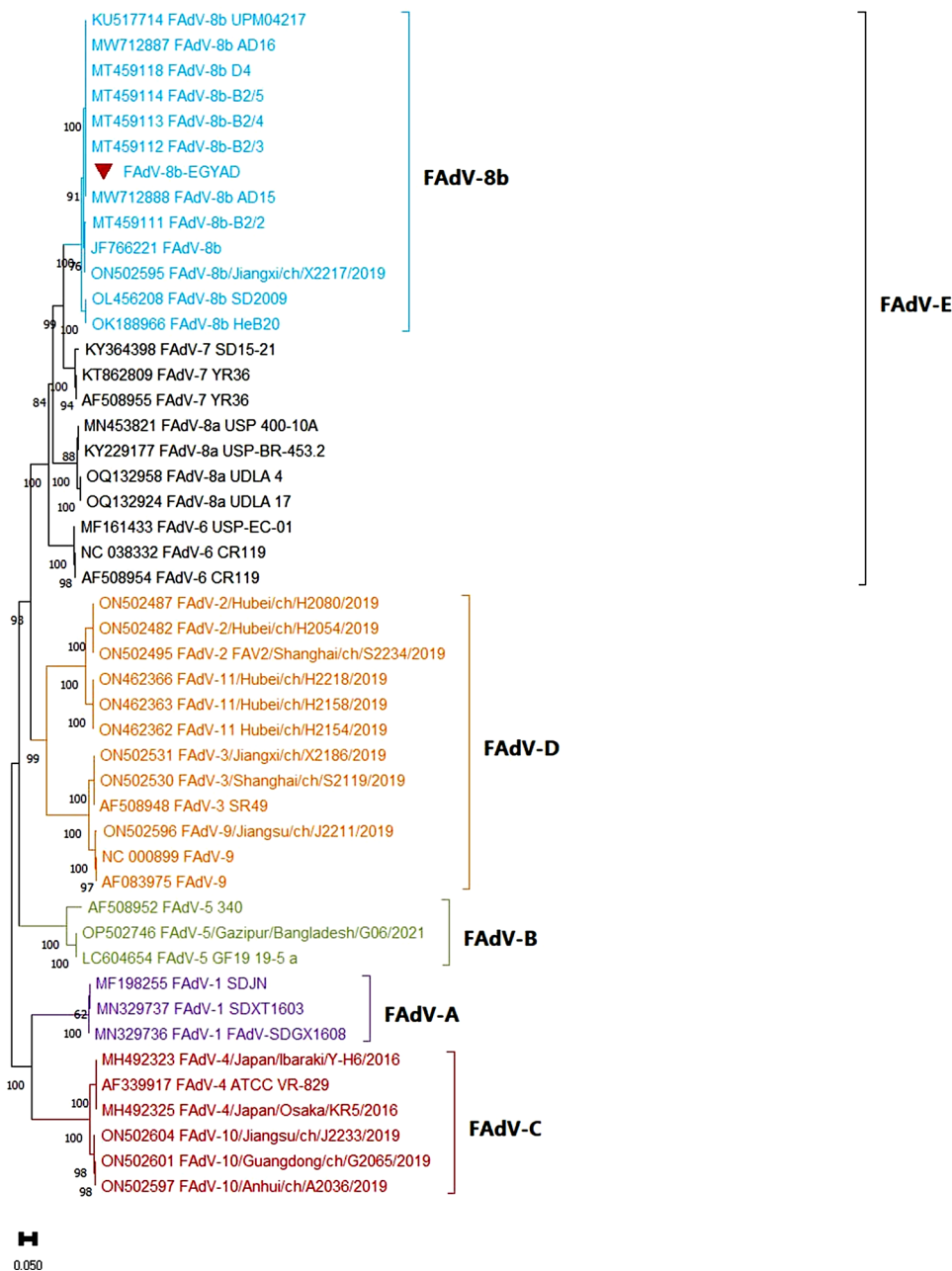
intestine had shortened villi with desquamation of enterocytes. Microscopic examination of immunostained formalin-fixed samples collected from birds that were adenovirus positive by PCR showed positive signals in the nuclei of interalveolar cells, enterocytes, and almost all hepatocytes (Fig. 9A-C).

## Discussion

Avian adenoviruses are important pathogens that infect a wide range of hosts. Their classification is complex, with evidence of crossing of species barriers and recombination



**Fig. 5** Phylogenetic analysis of adenoviruses based on the nucleotide sequences of the hexon gene. EGYAD is indicated by an inverted triangle.



and Maartens et al. [33], which, however, were performed on chickens.

Histopathological examination of the liver, intestine, lungs, trachea, heart, spleen, and kidney tissues from diseased birds yielded valuable information on the virulence and pathogenesis of the virus. The pathological results are consistent with previous studies [3, 32, 33]. There have not been many studies in which IHC was used to detect the virus in infected tissues, but in this study, we were able to demonstrate the presence of viral antigens in liver, lung, and intestinal tissues by IHC. Prominent lesions were found in the gastrointestinal tract and liver, and this may be due to the entry of the virus through the feco-oral route [4].

Hexon gene sequencing is generally considered sufficient for phylogenetic analysis, as this protein carries the major epitopes and provides information about genetic diversity. However, classification based on the hexon gene can be misleading if the virus undergoes interserotypic recombination. Therefore, for typing and subtyping, full-genome sequencing is more reliable. The fact that only the hexon region was examined is a major limitation of our study. Another is that the virus was not experimentally inoculated into turkeys to confirm its pathogenicity. However, its pathogenicity was suggested by our IHC results and the observation that none of the samples tested were positive for ??H5??, ??AOAV-1??, or ??aMPV??.

**Fig. 6** (A–D) Micrographs of H&E-stained formalin-fixed tissue samples collected from birds that were adenovirus positive by PCR, showing moderate hyperplasia of goblet cells with heterophils infiltration (black arrow) (A) in the trachea, congestion (arrowheads), haemorrhage (red arrow), perivascular fibrosis and fibrosis in the alveolar wall (thin black arrow), and multiple foci of leukocytic cells aggregation (thick arrow) in lungs (B–D)

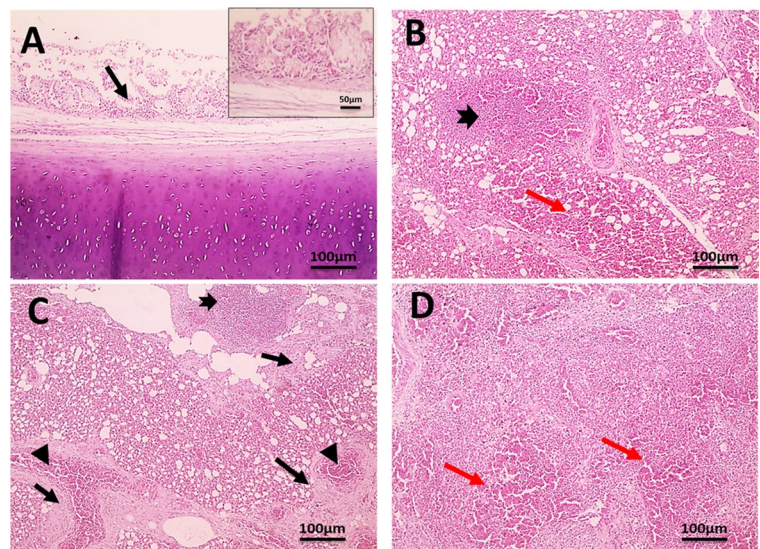
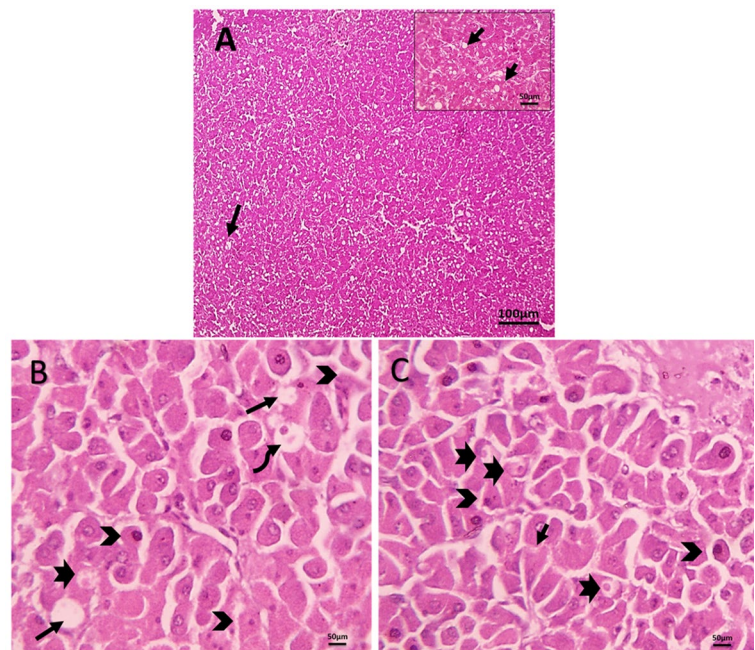


**Fig. 7** (A–C) Micrographs of H&E-stained liver samples collected from birds that were positive for adenovirus by PCR, showing fatty change in hepatocytes (thin black arrow) (A), eosinophilic and basophilic intranuclear (thick black arrow) inclusion bodies, nuclear pyknosis (arrow-head), and apoptotic bodies (curved black arrow)



## Conclusion

To our knowledge, this is the first study in which fowl adenovirus isolated from turkeys in Egypt was characterized. This study was designed to investigate adenovirus circulating in turkeys in the delta region of northern Egypt. Fowl adenovirus type 8b was discovered, suggesting that this rare serotype may be circulating in Egypt. More studies are needed to trace its origin and assess the risk posed by this virus.



**Fig. 8** (A-E) Micrographs of H&E-stained formalin-fixed tissue samples collected from birds that were adenovirus positive by PCR, showing depletion of lymphocytes from the white pulp (black arrow) in the spleen (A), interstitial edema (black arrow) in heart (B), marked interstitial edema, fibrosis (black arrow) (C), congestion (red arrow) in kidneys (D), and shortened villi with desquamation of enterocytes (black arrow) in the small intestine (E)

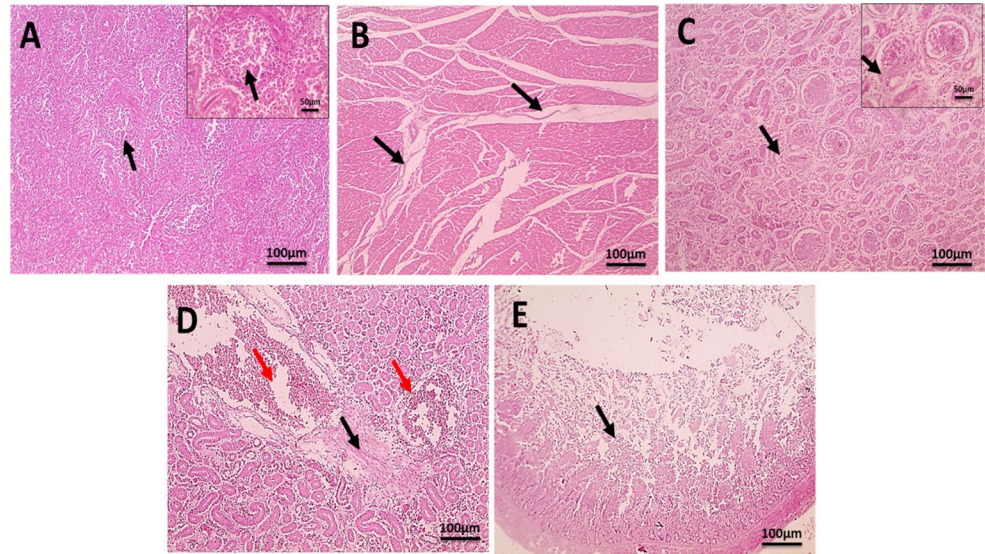
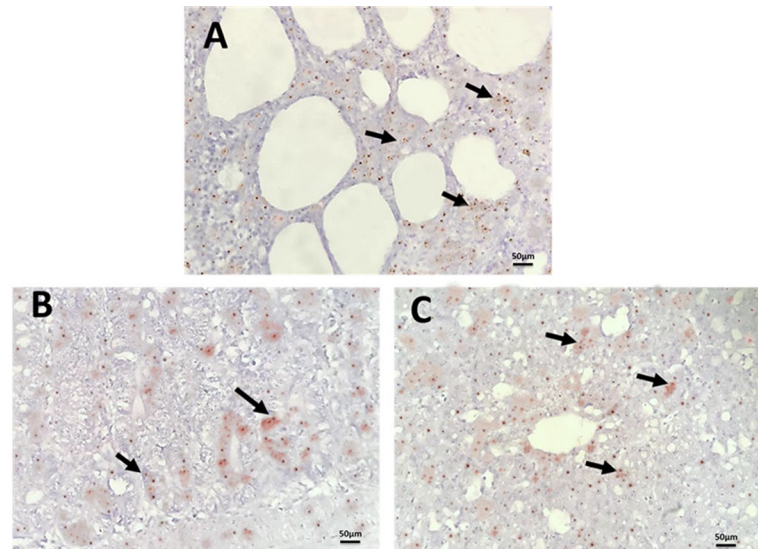


**Fig. 9** (A-C) Micrographs of formalin-fixed tissue samples collected from birds that were adenovirus positive by PCR and immunostained for the presence of viral antigen, showing positive brown staining (arrows) in the nuclei of interalveolar cells in lungs (A), enterocytes (B), and hepatocytes (C). The samples were counterstained with Mayer's haematoxylin



**Supplementary Information** The online version contains supplementary material available at <https://doi.org/10.1007/s00705-024-06057-9>.

**Acknowledgements** The authors thank the farm owners and workers for their help in collecting the data needed to conduct this study. We thank all participants involved in this project for their help, support, and advice.

**Author contributions** All of the authors contributed to the study conception and design. Material preparation, data collection, and analysis were performed by Shady Shalaby, Walaa Awadin, Sanaa Salem, Reham Karam, and Ahmed El-Shaieb. The first draft of the manuscript was written by Shady Shalaby, and all authors commented on previous versions of the manuscript. All authors read and approved the final manuscript.

**Funding** The authors declare that no funds, grants, or other support were received during the preparation of this manuscript.

**Data availability** The raw sequencing data obtained in this study were

submitted to the GenBank database (GenBank Overview (nih.gov)) under the accession number OR495594 and will be available online after publication.

## Declarations

**Ethical approval** This study was approved by the ethics committee of the faculty of veterinary medicine at Mansoura University. Code: Ph.D./100.

**Conflict of interest** The authors have no relevant financial or non-financial interests to disclose.

## References

1. Taylor KJM, Ngunjiri JM, Abundo MC, Jang H, Elaish M, Ghorbani A et al (2020) Respiratory and Gut Microbiota in Commercial Turkey Flocks with Disparate Weight Gain Trajectories Display Differential Compositional Dynamics. *Appl*

- Environmental Microbiol 86(12):e00431–e00420. <https://doi.org/10.1128/AEM.00431-20>
2. Scott D, Fitzgerald S, Rautenschlein HM, Mahsoub F, William Pierson WM, Reed, Jack SW (2020) Aviadonavirus Infections. In: Swayne DE (ed) Diseases of Poultry, 14th edn. Wiley, pp 322–332. <https://doi.org/10.1002/9781119371199.ch9>
  3. Shivaprasad HL, Woolcock PR, McFarland MD (2001) Group I avian adenovirus and avian adeno-associated virus in turkey poults with inclusion body hepatitis. Avian pathology: J WVPA 30(6):661–666. <https://doi.org/10.1080/03079450120092152>
  4. Rautenschlein S, Mahsoub HM, Fitzgerald SD, Pierson FW (2020) Hemorrhagic Enteritis and Related Infections. In: Swayne DE (ed) Diseases of Poultry, 14th edn. Wiley, pp 339–347. <https://doi.org/10.1080/03079457.2020.1794237>
  5. Benkó M, Aoki K, Arntberg N, Davison AJ, Echavarría M, Hess M et al (2022) ICTV Virus Taxonomy Profile: Adenoviridae 2022. J Gen Virol 103(3). <https://doi.org/10.1099/jgv.0.001721>
  6. Zhang J, Xie Z, Pan Y, Chen Z, Huang Y, Li L et al (2024) Prevalence, genomic characteristics, and pathogenicity of fowl adenovirus 2 in Southern China. Poult Sci 103(1):103177. <https://doi.org/10.1016/j.psj.2023.103177>
  7. Schachner A, Matos M, Graff B, Hess M (2018) Fowl adenovirus-induced diseases and strategies for their control – a review on the current global situation. Avian Pathol 47(2):111–126. <https://doi.org/10.1080/03079457.2017.1385724>
  8. Guy JS, Schaeffer JL, Barnes HJ (1988) Inclusion-body hepatitis in day-old turkeys. Avian Dis 32(3):587–590. <https://doi.org/10.2307/1590936>
  9. Itakura C, Yasuba M, Goto M (1974) Histopathological studies on inclusion body hepatitis in broiler chickens. Jap J vet Sci 36(4):329–335. <https://doi.org/10.1292/jvms1939.36.329>
  10. Guy JS, Barnes HJ (1997) Characterization of an avian adenovirus associated with inclusion body hepatitis in day-old turkeys. Avian Dis 41(3):726–731. <https://doi.org/10.2307/1592167>
  11. Ramsubeik S, Jerry C, Uzal FA, Stoute S (2023) Necrotic enteritis in a commercial turkey flock coinfecting with hemorrhagic enteritis virus. J veterinary Diagn investigation: official publication Am Association Veterinary Lab Diagnosticians Inc 35(3):317–321. <https://doi.org/10.1177/10406387231157711>
  12. Adel A, Mohamed AAE, Samir M, Hagag NM, Erfan A, Said M et al (2021) Epidemiological and molecular analysis of circulating fowl adenoviruses and emerging of serotypes 1, 3, and 8b in Egypt. Heliyon 7(12):e08366. <https://doi.org/10.1016/j.heliyon.2021.e08366>
  13. Falcone E, Tarantino M, Di Trani L, Cordioli P, Lavazza A, Tollis M (1999) Determination of bovine rotavirus G and P serotypes in Italy by PCR. J Clin Microbiol 37(12):3879–3882. <https://doi.org/10.1128/jcm.37.12.3879-3882.1999>
  14. Altschul SF, Gish W, Miller W, Myers EW, Lipman DJ (1990) Basic local alignment search tool. J Mol Biol 215(3):403–410. [https://doi.org/10.1016/S0022-2836\(05\)80360-2](https://doi.org/10.1016/S0022-2836(05)80360-2)
  15. Tamura K, Stecher G, Kumar S (2021) MEGA11: Molecular Evolutionary Genetics Analysis Version 11. Mol Biol Evol 38(7):3022–3027. <https://doi.org/10.1093/molbev/msab120>
  16. Tajima F, Nei M (1984) Estimation of evolutionary distance between nucleotide sequences. Mol Biol Evol 1(3):269–285. <https://doi.org/10.1093/oxfordjournals.molbev.a040317>
  17. Thompson JD, Higgins DG, Gibson TJ (1994) CLUSTAL W: improving the sensitivity of progressive multiple sequence alignment through sequence weighting, position-specific gap penalties and weight matrix choice. Nucleic Acids Res 22(22):4673–4680. <https://doi.org/10.1093/nar/22.22.4673>
  18. Sievers F, Higgins DG (2014) Clustal omega. Curr protocols Bioinf 48(1):3131–3136. <https://doi.org/10.1002/0471250953.bi0313s48>
  19. Slaoui M, Fiette L (2011) Histopathology procedures: from tissue sampling to histopathological evaluation. Drug safety evaluation. Springer, pp 69–82. [https://doi.org/10.1007/978-1-60761-849-2\\_4](https://doi.org/10.1007/978-1-60761-849-2_4)
  20. Suvarna K, Layton C, Bancroft J (2019) Bancroft's Theory and Practise of Histological Techniques (8th edition): Elsevier; <https://doi.org/10.1016/C2015-0-00143-5>
  21. Kim S-W, Roh J, Park C-S (2016) Immunohistochemistry for Pathologists: Protocols, Pitfalls, and Tips. J Pathol Transl Med 50(6):411–418. <https://doi.org/10.4132/jptm.2016.08.08>
  22. Radwan MM, El-Deeb AH, Mousa MR, El-Sanousi AA, Shalaby MA (2019) First report of fowl adenovirus 8a from commercial broiler chickens in Egypt: molecular characterization and pathogenicity. Poult Sci 98(1):97–104. <https://doi.org/10.3382/ps/pey314>
  23. Tykałowski B, Śmiałek M, Koncicki A, Ognik K, Zduńczyk Z, Jankowski J (2019) The immune response of young turkeys to haemorrhagic enteritis virus infection at different levels and sources of methionine in the diet. BMC Vet Res 15(1):1–11. <https://doi.org/10.1186/s12917-019-2138-8>
  24. Haunshi S, Sharma D (2002) Immunocompetence in native and exotic chicken populations and their crosses developed for rural farming. Indian J Poult Sci 37(1):10–15. <https://doi.org/10.18805/IJAR.B-4890>
  25. El-Sayed A, Kamel M (2020) Climatic changes and their role in emergence and re-emergence of diseases. Environ Sci Pollut Res Int 27(18):22336–22352. <https://doi.org/10.1007/s11356-020-08896-w>
  26. Ebner K, Pinsker W, Lion T (2005) Comparative sequence analysis of the hexon gene in the entire spectrum of human adenovirus serotypes: phylogenetic, taxonomic, and clinical implications. J Virol 79(20):12635–12642. <https://doi.org/10.1128/jvi.79.20.12635-12642.2005>
  27. Elbestawy AR, Ibrahim M, Hammam H, Noreldin AE, Bahrawy AE, Ellakany HF (2020) Molecular Characterization of Fowl Adenovirus D Species in Broiler Chickens with Inclusion Body Hepatitis in Egypt. alexandria J veterinary Sci 64:110–117. <https://doi.org/10.5455/ajvs.74411>
  28. Rasmussen UB, Schlesinger Y, Pavirani A, Mehtali M (1995) Sequence analysis of the canine adenovirus 2 fiber-encoding gene. Gene 159(2):279–280. [https://doi.org/10.1016/0378-1119\(95\)00110-r](https://doi.org/10.1016/0378-1119(95)00110-r)
  29. Mansoor MK, Hussain I, Arshad M, Muhammad G (2011) Preparation and evaluation of chicken embryo-adapted fowl adenovirus serotype 4 vaccine in broiler chickens. Trop Anim Health Prod 43(2):331–338. <https://doi.org/10.1007/s11250-010-9694-z>
  30. Cizmeçigil UY, Umar S, Yilmaz A, Bayraktar E, Turan N, Tali B et al (2020) Characterisation of fowl adenovirus (FAdV-8b) strain concerning the geographic analysis and pathological lesions associated with inclusion body hepatitis in broiler flocks in Turkey. J Veterinary Res 64(2):231. <https://doi.org/10.2478/jvetres-2020-0026>
  31. Kefford B, Borland R, Slattery JF, Grix DC (1980) Serological identification of avian adenoviruses isolated from cases of inclusion body hepatitis in Victoria, Australia. Avian Dis 24(4):998–1006. <https://doi.org/10.2307/1589974>
  32. El-Shall NA, El-Hamid HSA, Elkady MF, Ellakany HF, Elbestawy AR, Gado AR et al (2022) Epidemiology, pathology, prevention, and control strategies of inclusion body hepatitis and hepatitis-hydropericardium syndrome in poultry: A comprehensive review. Front Vet Sci 9. <https://doi.org/10.3389/fvets.2022.963199>
  33. Maartens LH, Joubert HW, Aitchison H, Venter EH (2014) Inclusion body hepatitis associated with an outbreak of fowl adenovirus type 2 and type 8b in broiler flocks in South Africa. J S Afr Vet Assoc 85(1):e1–5. <https://doi.org/10.4102/jsava.v85i1.1146>

**Publisher's Note** Springer Nature remains neutral with regard to jurisdictional claims in published maps and institutional affiliations.

Springer Nature or its licensor (e.g. a society or other partner) holds exclusive rights to this article under a publishing agreement with the author(s) or other rightsholder(s); author self-archiving of the accepted manuscript version of this article is solely governed by the terms of such publishing agreement and applicable law.